Macromolecules **2001,** *34,* 9189−9192

Notes

Modeling the Barrier Properties of Polymer-Layered Silicate Nanocomposites

R. K. Bharadwaj

Avery Research Center, 2900 Bradley Street,
Pasadena, California 91107

Received May 7, 2001
Revised Manuscript Received July 12, 2001

Introduction

Polymer-layered silicate nanocomposites belong to an emerging class of organic−inorganic hybrid materials that show promise as barrier materials for a multitude of packaging applications.[1,2] Demonstrated improvements in the gas barrier properties at low concentrations of the layered silicate (<5 wt %) have been reported in polyimide,[3,4] polycaprolactone,[5] and poly(vinyl alcohol)[6] matrices, while simultaneously imparting improved mechanical, thermal, and flame resistance properties. Nanoscopic dispersion of the layered silicate in a polymer matrix results in a greater enhancement in gas barrier property compared to conventional phase-separated composites.[1−6]

Layered silicates (clays) are crystalline materials consisting of 1 nm thick layers (or sheets) which are made up of an octahedral sheet of alumina sandwiched between two tetrahedral sheets of silica. The length of the individual sheets can range from 30 to ∼2000 nm depending on the particular silicate. Spacing between the sheets is mediated by the presence of surfactants or ions that balance the net negative charge present in the sheets due to isomorphic substitutions. Three possibilities arise upon blending layered silicates with a polymer through solution, melt, or in-situ polymerization routes. The polymer-layered silicate combination may be immiscible in which event a conventional *phase-separated* composite results. The other two possibilities are *intercalation*, where the polymer chains swell the intersheet or gallery spacing and lead to a well-ordered alternating polymer−silicate-layered nanostructure, and *exfoliation*, where the silicate sheets are completely delaminated and individually dispersed in the polymeric matrix. The latter two morphologies involve nanoscale interactions between the polymer and silicate that give rise to many of the appealing properties discussed above.

Although the enhancements in gas barrier properties are well-known in polymer−silicate nanocomposites, its dependence on factors such as the relative orientation of the sheets in the matrix and the state of aggregation and dispersion (intercalated, exfoliated, or some intermediate) are not well understood. The present study addresses both of these issues by modifying a simple model developed to describe permeability in filled polymers on the basis of tortuosity arguments.[7] The correlation between the sheet length, concentration, relative orientation, and state of aggregation is expected to provide guidance in the design of better barrier materials using the nanocomposite approach.

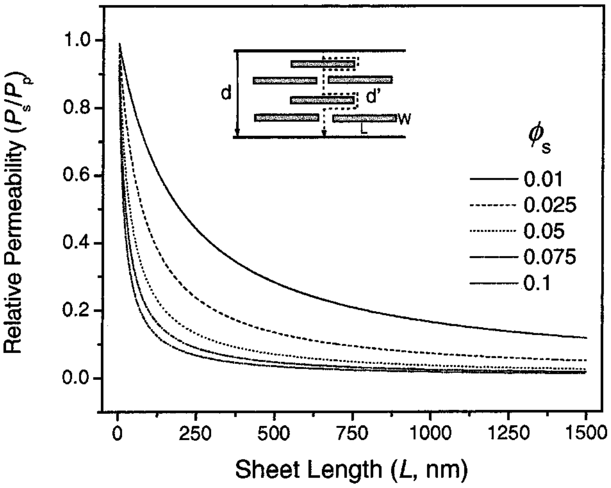

Figure 1. Dependence of the relative permeability on the sheet length at several different volume fractions of the silicate as obtained from eq 2. The inset is an illustration of the tortuosity for a diffusing penetrant introduced upon exfoliating layered silicates in a polymer matrix.

Model

We invoke a simple model developed to describe the permeability in filled polymers.[7] The model strives to predict the observed permeability based strictly on tortuosity arguments. The presence of a filler (spherical, plate, cylindrical, etc.) introduces a tortuous path for a diffusing penetrant. The reduction of permeability arises from the longer diffusive path that the pentrants must travel in the presence of the filler (layered silicate in the present case) and is illustrated in the inset in Figure 1. A sheetlike morphology is particularly efficient at maximizing the path length due to the large length-to-width ratio compared to other shapes of filler such as spheres or cubes. The tortuosity factor (τ) is defined as the ratio of the actual distance (d') that a penetrant must travel to the shortest distance (d) that it would have traveled in the absence of the layered silicate and is expressed in terms of the length (L), width (W), and volume fraction of the sheets (ϕ_s) as

$$\tau = \frac{d'}{d} = 1 + \frac{L}{2W}\phi_s \tag{1}$$

The effect of tortuosity on the permeability is expressed as

$$\frac{P_s}{P_p} = \frac{1 - \phi_s}{\tau} \tag{2}$$

where P_s and P_p represent the premeabilities of the

10.1021/ma010780b CCC: $20.00

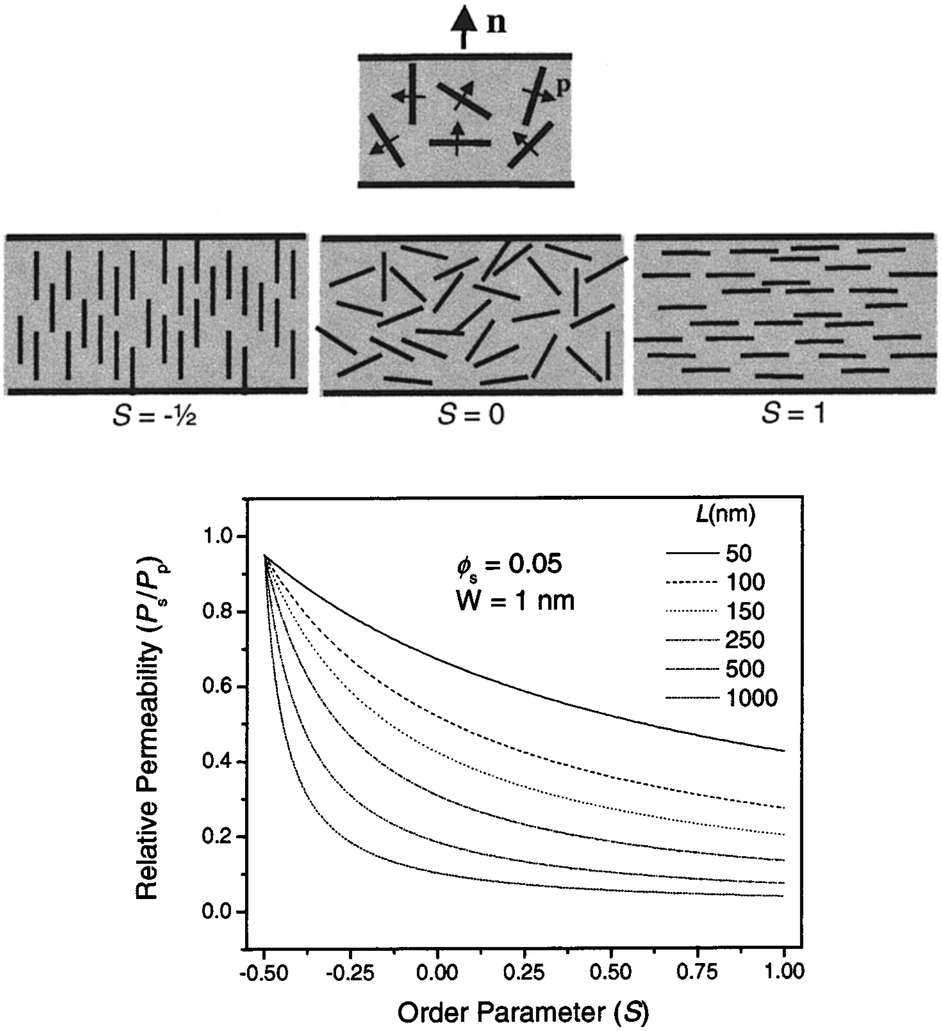

Figure 2. Effect of sheet orientation on the relative permeability in exfoliated nanocomposites at $\phi_s = 0.05$ and $W = 1$ nm. The illustrations show the definition of the direction of preferred orientation (**n**) of the silicate sheet normals (**p**) with respect to the film plane. Illustrations for three values of the order parameter (S) $-^1/_2$, 0, and 1 are also shown.

polymer–silicate nanocomposite and pure polymer, respectively. In the present case, the polygonal aluminosilicate sheets are approximated as disks with a mean diameter L ranging from 30 to 2000 nm with a width of 1 nm.

Although eq 2 was developed to model the diffusion in filled polymers (conventional composites), it surprisingly does extremely well in tracking the experimental results for relative permeability in polymer–clay nanocomposites. In a detailed study,[3,4] polyimide nanocomposites with 2 wt % of several different silicates (hectorite, saponite, montmorillonite, and synthetic mica) were prepared and H_2O permeability was measured. The average length of the individual clay sheets ranged from ~46 nm in hectorite, 165 nm in saponite, 218 nm in montmorillonite, and 1230 nm in synthetic mica. Water permeability was reduced by a factor of 10 over the pure polyimide by dispersing 2 wt % of synthetic mica. The model predictions from eq 2 tracked the relative permeability as a function of the silicate sheet length closely. In addition, eq 2 was also found to accurately reproduce the observed concentration dependence of the relative permeability of H_2O in polyimide–montmorillonite nanocomposite.[3]

Relative permeabilities at several different silicate volume fractions are shown in Figure 1 as a function of sheet length based on eq 2. The curves are gradually displaced to progressively lower relative permeabilities as a function of increasing concentration and sheet length. This is to be expected given the extremely large length-to-width ratio of silicate sheets (30 to ~2000 nm in length, 1 nm thick) that serves to significantly increase the tortuosity. Also, there is not a significant reduction in the relative permeability regardless of sheet length beyond $\phi_s = 0.05$. This is in agreement with experimental observations where the enhancements typically occur at very low silicate concentrations.[1-6]

Effect of Sheet Orientation

The model described herein makes a key assumption that the sheets are placed such that the sheet normal is coincident with the direction of diffusion. Clearly, this arrangement of the sheets results in the highest tortuosity. Any deviation from the arrangement where the sheet normals lie perpendicular to the film plane would in fact lead to deterioration in the barrier properties. A range of relative orientations of the sheets with respect to each other and the plane of the film may be envisaged as illustrated in Figure 2. The two extremes, planar and orthogonal alignment of the sheets, may be treated by simply interchanging L and W in eq 1. However, considering that a range of orientations are possible, it would be more instructive to modify eq 1 to consider the dependence of the tortuosity factor on the orienta-

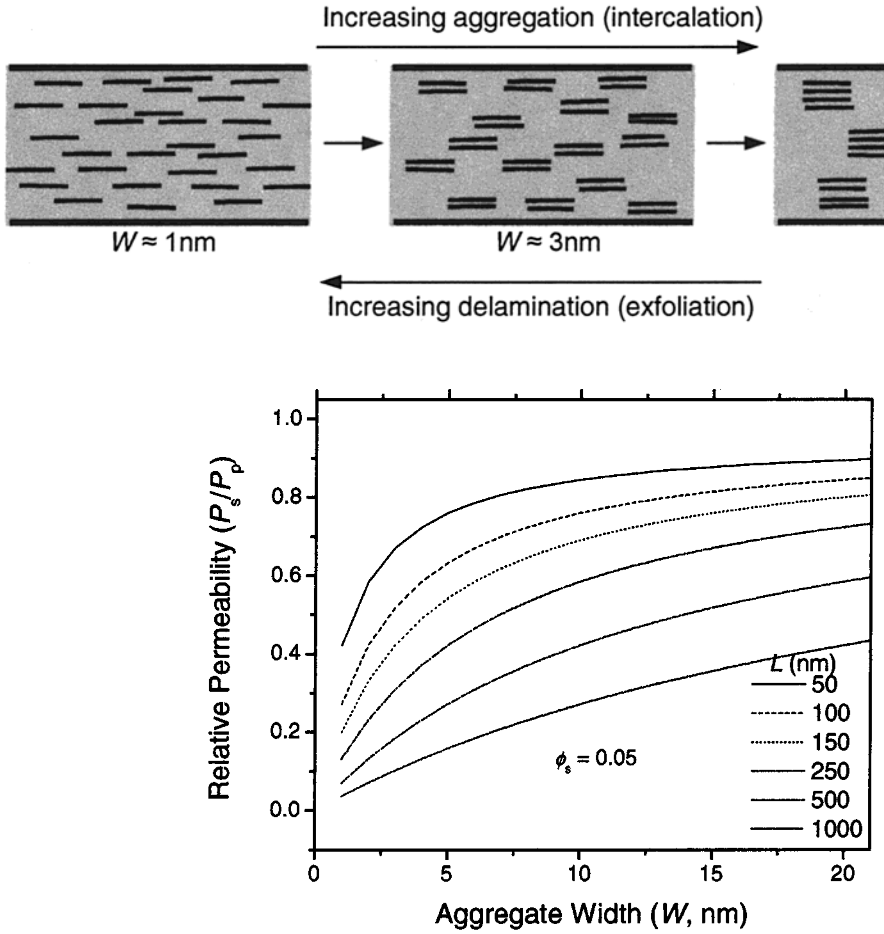

Figure 3. Effect of incomplete exfoliation on the relative permeability. The illustrations show the effect of having one, two, and four sheet aggregates dispersed throughout the matrix. The plot shows the relative permeability as a function of the aggregate width at several different lengths of the sheets at $\phi_s = 0.05$.

tional order of the sheets in a continuous manner. The order parameter[8] (S) presents a convenient framework within which this can be achieved and is defined as

$$S = \frac{1}{2}\langle 3\cos^2\theta - 1\rangle \qquad (3)$$

where θ represents the angle between the direction of preferred orientation (**n**) and the sheet normal (**p**) unit vectors as shown in Figure 2. This function can range from 1 ($\theta = 0$), indicating perfect orientation of the sheet normal unit vectors **p** with **n**, to $-{}^1/_2$ ($\theta = {}^{\pi}/_2$), indicating perpendicular or orthogonal orientation, and a value of 0, indicating random orientation of the sheets. The angular brackets denote averaging over all the sheets in the system. The tortuosity factor is modified to include the orientational order, and the relative permeability is given by

$$\frac{P_s}{P_p} = \frac{1-\phi_s}{1+\frac{L}{2W}\phi_s\left(\frac{2}{3}\right)\left(S+\frac{1}{2}\right)} \qquad (4)$$

The above expression reduces to eq 2 when $S = 1$ (planar arrangement) and converges approximately to the permeability of the pure polymer when $S = -{}^1/_2$ (orthogonal arrangement) as illustrated in Figure 2. We note that when the sheets are arranged orthogonal to the plane of the film, the permeability given by the above expression coincides with the exact solution given by interchanging L and W in eq 1 (i.e., $\tau = (W/2L)\phi_s$), only in the limit $W \ll L$. This is a reasonable approximation given that the aluminosilicate sheets satisfy the limit W (~1 nm) $\ll L$ (~30−1000 nm) in the range of interest. It is to be expected that the barrier property is enhanced when $S = 1$ and decays in a continuous fashion as predicted by eq 4 to nearly that of the pure polymer when $S = -{}^1/_2$ where the sheets are arranged such that there is negligible increase in the tortuosity as shown in Figure 2. Shorter sheets, by virtue of the small L to W ratio, are very sensitive to orientational order. A small random rotation of the sheet normals from the direction of preferred orientation is sufficient to degrade the barrier properties significantly as shown in Figure 2. In contrast, as the sheet length increases, the increase in the L to W ratio helps in reducing the dependence on the relative orientation. Long sheets mitigate the effect of rotating the plane of the sheets with respect to the plane of the film on the tortuosity. For $L > 500$ nm, the barrier property degrades only in the range $-{}^1/_2 \leq S \leq 0$ at $\phi_s = 0.05$. Therefore, incorporating sheets with $L > 500$ nm is beneficial, in that the enhancement in barrier property with a random orientation of the sheets is nearly as good as the case where the sheets were aligned perpendicular to the diffusing path.

State of Delamination

Much of the expected improvement in polymer-layered silicate nanocomposites is predicated on complete layer delamination and dispersion. Experimentally,[1,2] with a few exceptions this is rarely achieved. A state of delamination intermediate to intercalation and exfoliation is observed more often than not. For example, a situation wherein stacks of intercalated aggregates are dispersed throughout the matrix may be envisaged. It is important to note that in this latter case, where complete layer delamination and dispersion does not occur, the predicted enhancement in barrier property based on dispersion of individual sheets is no longer valid. Aggregation through intercalation serves to increase the effective width of the nanocomposite. That is, polymer nanocomposites can adopt variable widths depending on the extent of delamination. By way of illustration, consider single sheets of silicate dispersed in a matrix. Here the width is ~1 nm, and this serves to maximize the L to W ratio. In contrast, consider a case where aggregates comprised of two silicate sheets with a layer of polymer in between dispersed throughout the matrix. Now, the width increases to ~3 nm assuming that the polymer layer is 1 nm thick. Taking this concept further, aggregates of four silicate sheets with three layers of polymer chains in between lead to an effective width of ~7 nm. In Figure 3, the effect of increasing aggregation or decreasing delamination while keeping the sheets parallel to the film plane is illustrated. In each case, the same number of sheets and sheet length are shown. In the first case, single sheets are dispersed throughout resulting in an ideal structure. Dispersing the same total number of sheets as two-sheet aggregates results in a dramatic decrease in the tortuosity. Aggregates of four silicate sheets begin to show a percolating path for the diffusing penetrant. The above argument can be extended to include the lateral displacement of the sheets with respect to each other while maintaining a regular stacking arrangement leading to a variability in the length of the aggregate in addition to the width.

Clearly, exfoliation appears to be the critical factor in determining the maximum performance of polymer nanocomposites for barrier applications. In Figure 3, the relative permeability is plotted as a function of increasing width, W, that results from the formation of aggregates at several different lengths of the silicate sheet (at $\phi_s = 0.05$). As seen, relative permeability is extremely sensitive to incomplete delamination. This is especially true for the short sheet lengths. At $L = 1000$ nm, the expected relative permeability is ~0.05 for $W = 1$ nm and degrades to 0.2 for $W = 7$ nm. In the same W range but for $L = 500$ nm, P_c/P_p degrades from 0.1 to 0.4 underscoring the need for complete exfoliation of the silicate sheets.

Conclusions

The effects of sheet length, concentration, orientation, and degree of delamination on the relative permeability have been explored by modifying a simple tortuosity-based model. Dispersing longer sheets ($L > 500$ nm) in a polymer matrix is particularly beneficial in several respects by (1) increasing the tortuosity, (2) reducing the dependence of the relative permeability on the orientational order of the sheets, and (3) slowing the degradation in barrier property with decreasing state of delamination, i.e., increasing aggregation via intercalation. The last of these factors ultimately controls the barrier properties of polymer-layered silicate nanocomposites.

Acknowledgment. The author sincerely acknowledges the partial funding of this work by the NIST/Advanced Technology Program.

References and Notes

(1) Giannelis, E. P.; Krishnamoorti, R.; Manias, E. *Adv. Polym. Sci.* **1999**, *138*, 107.
(2) LeBaron, P. C.; Wang, Z.; Pinnavaia, T. J. *Appl. Clay Sci.* **1999**, *15*, 11.
(3) Yano, K.; Usuki, A.; Okada, A.; Kuruachi, T.; Kamigaito, O. *J. Polym. Sci., Part A* **1993**, *31*, 2493.
(4) Yano, K.; Usuki, A.; Okada, A. *J. Polym. Sci., Part A* **1997**, *35*, 2289.
(5) Giannellis, E. P. *Adv. Mater.* **1996**, *8*, 29.
(6) Strawhecker, K. E.; Manias, E. *Chem. Mater.* **2000**, *12*, 2943.
(7) Nielsen, L. E. *J. Macromol. Sci., Chem.* **1967**, *A1*, 929.
(8) Chandrasekhar, S. *Liquid Crystals*, 2nd ed.; Cambridge University Press: New York, 1992.

MA010780B